

Available online at www.sciencedirect.com**SciVerse ScienceDirect**

Procedia Engineering 42 (2012) 824 – 832

**Procedia
Engineering**

www.elsevier.com/locate/procedia

20th International Congress of Chemical and Process Engineering CHISA 2012
25 – 29 August 2012, Prague, Czech Republic

Heat transfer in a granular media modeled by a coupled DEM-Finite difference method: application to fluidized bed processes

V-D. Nguyen ^a*, K. Benhabib, C. Marie, P. Coorevits

*Université de Picardie Jules Verne, Eco-PRocédés, Optimisation et Aide à la Décision, (EPROAD EA 4669),
IUT de l'Aisne, 48 rue d'Ostende, F-02100 Saint Quentin – France*

Abstract

The aim of this study is to simulate the heat transfer in a granular media. It's a phenomenon found, for example, in the convective drying in chemicals, pharmaceuticals industry or in the powder metallurgy... The temperature field of the granular phase is modelled by the Discrete Elements Method (DEM) and coupled to the fluid or solid phase one, which is modelled by finite difference method. The emphasis is placed on the heat transfer between particles in contact (conductance) and convection solid/fluid. Process examples during several hours can be simulated by our coupled method. Various comparisons with experimental results are presented to validate the model.

© 2012 Published by Elsevier Ltd. Selection under responsibility of the Congress Scientific Committee (Petr Kluson) Open access under [CC BY-NC-ND license](https://creativecommons.org/licenses/by-nc-nd/4.0/).

Key-words: Heat transfer; DEM; coupling DEM-finite difference method

1. Introduction

The principal objective of this work is to study heat transfer in a granular media. Firstly, the domain of application is in process engineering, chemicals, pharmaceuticals industry... Recently, Janas *et al.* [1] studied the drying of a maize bed by an empirical model, which doesn't describe the temperature

* Corresponding author. Tel.: +33 323 503 692.

E-mail address: vietdung.nguyen@u-picardie.fr

evolution at the local level. Furthermore, Tang *et al.* [2] presented a simple model for the drying of a fixed bed of food product with superheated steam. They considered that the bed is divided into three zones (dry zone, progress zone and wetland zone). However, the studies of Hager *et al.* [3], Kato *et al.* [4] are interested in hybrid models based on the average theory or semi-empirical models. In the literature, only few studies were interested to understanding these phenomena at the local level by using the DEM. Vargas [5] examined experimentally and numerically the heat transfer models in a granular media. Simsek *et al.* [6] studied this phenomenon in a grate firing system.

In this paper, we study initially the heat transfer in the granular solid phase. In a second step, we present the thermal interaction in solid-fluid phases and finally, we focus on validation with experimental and numerical results reported in the literature.

2. Heat transfer modelling

2.1. Heat transfer in granular media

The modelling of heat transfer by conduction, by convection and heat generation by friction has been detailed and validated previously by Nguyen *et al* [7].

In agreement with this study, the temperature increase of a particle Ω_i is related to the dissipation of mechanical energy on heat, to the heat transfer by contact with neighbouring bodies and the convective transfer with the environment. Thus, the energy balance of a particle Ω_i which is in contact with α particles Ω_j is given by the expression

$$m_i C_p \frac{dT_i}{dt} = \sum_{j=1}^{\alpha} \left(H_C^{ij} (T_j - T_i) + \frac{1}{2} \Phi_{\mu}^{ij} \right) + \Phi_v^i \quad (1)$$

where m_i , C_p , and Φ_v^i are the mass, the heat capacity for Ω_i , the convective flux respectively.

- H_C^{ij} denotes contact conductance estimated from the Hertz theory for two-dimensional case as

$$H_C^{ij} = 2\lambda \sqrt{2aL_C} = 2\lambda \left(\frac{8r_n^{ij} a^*}{\pi E^*} \right)^{\frac{1}{4}} \quad (2)$$

for three-dimensional case (spherical particle)

$$H_C^{ij} = 2\lambda a = 2\lambda \left(\frac{3r_n^{ij} a^*}{4E^*} \right)^{\frac{1}{3}} \quad (3)$$

where λ the solid conductivity, L_C the length of the cylinder (1m in this study). a represents the radius of contact area and r_n is the normal force. a^* is the equivalent radius and E^* represents the effective Young's modulus.

- Φ_{μ}^{ij} is the heat dissipation by friction, which is proportional to sliding velocity \dot{u}_t^{ij} and tangential contact reaction r_t^{ij}

$$\Phi_{\mu}^{ij} = \dot{u}_t^{ij} r_t^{ij} \quad (4)$$

- Beside the heat conduction, convective heat flows from granular media into ambient air have to be taken into account. The convective flow Φ_v^i is expressed by

$$\Phi_v^i = h^i S_S (T_i - T_a) \quad (5)$$

where h^i is the heat transfer coefficient, S_S is the convective surface and T_a is ambient temperature.

In general, Equation (1) is solved with a small time step to assume that the heat transfer resistance through a particle Ω_i (conduction) is significantly lower than the contact resistance between two particles Ω_i and Ω_j . The second condition is that the temperature of each particle changes slowly, so that thermal perturbations do not propagate further than its immediate neighbours during one time step, provided that

$$\frac{\Delta t H_c}{m C_p} \ll 1. \quad (6)$$

2.2. Heat transfers in an interaction granular media/fluid

We study a granular bed embedded in a fluid having a fluidization velocity U_f along the Oy direction (Fig. 1). The system is divided into horizontal intervals homogeneous (REV) along the Oy direction. Each REV may contain several particles or parts of particle.

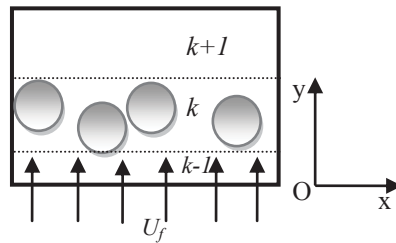


Fig. 1. Model of heat transfers in granular/fluid interaction.

The energy balance of a REV numbered k , which is in contact with neighbouring REV $k+1$ and $k-1$ is written

$$m_k^f C_p^f \left(\frac{\partial T_k^f}{\partial t} + U_k^f \frac{\partial T_k^f}{\partial y} \right) = \lambda^f S^f \frac{\partial^2 T_k^f}{\partial y^2} + \sum_{i=1}^{\gamma} h^f S_s^f (T_{i,k} - T_k^f) \quad (7)$$

where m_k^f , S^f , C_p^f , λ^f are respectively the fluid mass contained in REV, the fluid surface perpendicular with Oy direction, the heat capacity and the heat conductivity of fluid. S_s^f represents surface of particles in contact with the fluid located in this REV, $T_{i,k}$ is the particle temperature, T_k^f fluid temperature supposed constant in each REV.

By using centered finite difference method, we can write

$$m_k^f C_p^f \left(\frac{T_k^{f,t+\Delta t} - T_k^{f,t}}{\Delta t} + U_k^f \frac{T_{k+1}^{f,t} - T_k^{f,t}}{\Delta y} \right) = \lambda^f S^f \frac{T_{k+1}^{f,t} - 2T_k^{f,t} + T_{k-1}^{f,t}}{\Delta y^2} + \sum_{i=1}^{\gamma} h^f S_s^f (T_{i,k}^t - T_k^{f,t}) \quad (8)$$

So that

$$T_k^{f,t+\Delta t} = T_k^{f,t} + \frac{\lambda^f S^f \Delta t}{m_k^f C_p^f \Delta y^2} (T_{k+1}^{f,t} - 2T_k^{f,t} + T_{k-1}^{f,t}) + \frac{\Delta t \sum_{i=1}^{\gamma} h^f S_s^f (T_{i,k}^t - T_k^{f,t})}{m_k^f C_p^f} - \frac{\Delta t U_k^f}{m_k^f C_p^f \Delta y} (T_{k+1}^{f,t} - T_k^{f,t}) \quad (9)$$

Note that $T_0^{f,t}$ is the fluid temperature at model inlet. At the outlet, we consider that $T_n^{f,t}$ is equal to $T_{n-1}^{f,t}$.

3. Results and discussions

3.1. Validation of heat transfer by conductance

In order to validate our conductance model, we have compared the results with experimental data from Yun and Santamarina's work [8]. The experimental setup, as shown schematically in figure 2-a, consisted of a column of 15 aluminum-bronze spheres of same diameter of 25.4 mm arranged vertically in a tube. The parameters are shown in Table 1. The system is heated by an iron bar at 103 °C. A thermal capture of numerical model is presented in figure 2-b.

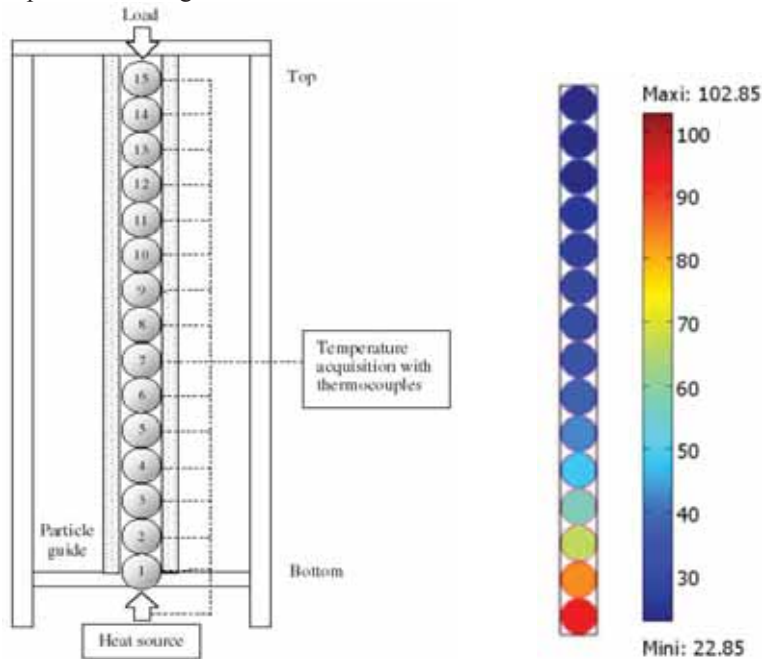


Fig. 2. (a) Experimental setup [8] (b) Numerical model

Table 1. Properties of aluminum-bronze spheres

Property	Value
Density [kg/m ³]	7500
Heat conductivity [W/(m.K)]	39.1
Heat capacity [J/(kg.K)]	400
Young's modulus [GPa]	70

The complexity of the problem and the absence of experimental characterization does not allow us to determine the experimental values of the conductance H_C and the coefficient of heat transfer by convection h . We will then determine these parameters for that the experimental heat evolution of the first particle matches the numerical evolution. A heat conductance of 0.06 W/mK and a coefficient of convective heat transfer 1.5 W/m²K were characterized.

From the thermal point of view, this simple example allows us to study the diffusion of the heat flow by conductance in granular media. In order to check that this assumption is not too restrictive, we

compared numerical prediction with the experimental results (see Fig. 3). Through this comparison, we could check that the thermal resistance within particles was negligible compared to the thermal contact resistance between particles. This hypothesis could be checked by studying the temperature evolution in particles 1, 2 and 3. The good agreement seems to validate the assumption about the heat transfer occurring by conductance.

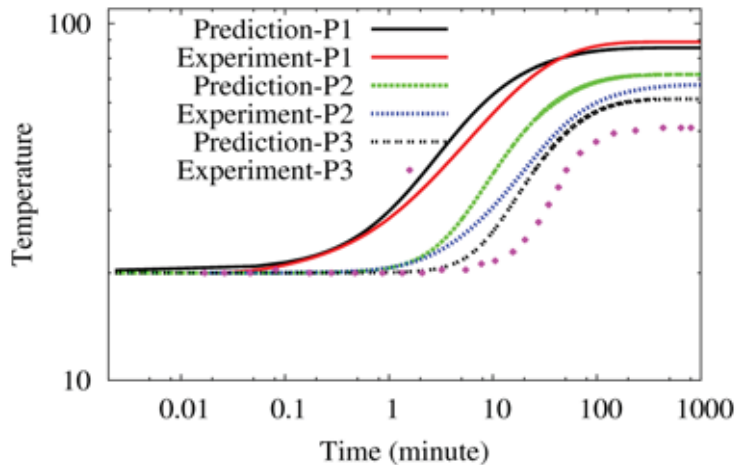


Fig. 3. Temperature evolution in particles 1, 2, and 3

Another validation based on experimental work [5]. In his studies, Vargas developed an experimental setup to investigate the heat transfer in a quasi-static configuration. The system is composed of dispersed stainless steel spheres forming a 3D packed bed ($0.3 \times 30.4 \times 45 \text{ cm}^3$). The bottom wall is kept at 50°C . The top, left and right walls are insulated. The initial temperature is 25°C . One-dimensional loading (1650 N) is imposed on the upper wall. In this vacuum system, only heat transfer by conductance is examined. The thermo mechanical properties of stainless steel based on experiments are detailed in Table 2.

Table 2. Parameters used in the simulation

Property	Value
Particle number	15549
Particle diameter [mm]	3
Poisson's ratio	0.29
Density [kg/m^3]	7500
Heat conductivity [W/(m.K)]	15
Heat capacity [J/(kg.K)]	440
Young's modulus [GPa]	193

In Figure 4-a, we present a thermal map after 30 minutes heating. The temperature in the heated granular bed does not propagate uniformly. The front oscillates as force chains appear and disappear along the bed's height. Figure 4-b shows a comparison of the temperature as a function of bed's height given by our predictions and the experimental results obtained by Vargas after 30 minutes heating. It can be seen

that the simulation result matches the experimental curve, which allows us to validate the model prediction in the quasi-static case.

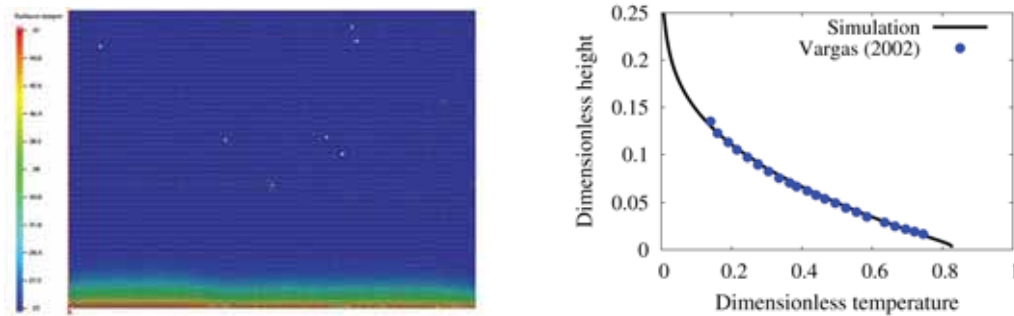


Fig. 4. (a) Thermal map after 30 minutes heating (b) and comparison of experimental data with numerical results

3.2. Validation of heat transfers modelling for a solid/fluid media

This part examines a heating problem of granular material studied experimentally by Simsek *et al.* [6]. An inert fixed bed is filled in a box (225 x 190 mm²). The material parameters are detailed in Table 3. Hot air enters at the bottom and flows up through the granular bed. Note that the fluidization velocity at the inlet of packed bed is determined by the ratio of air mass flow rate (in 3D) to the air density and to the cross section of particles bed.

Table 3. Properties of the materials

Property	Value
Mass [kg]	6
Bed height [mm]	190
Particle diameter [mm]	12.6
Particle density [kg/m ³]	1440
Particle heat conductivity [W/(m.K)]	0.16
Particle heat capacity [J/(kg.K)]	104.43
Air mass flow rate [kg/h]	16
Air temperature [°C]	200-300
Air heat conductivity [W/(m.K)]	0.0234
Air heat capacity [J/(kg.K)]	1055
Air viscosity [m ² /s]	18.10 ⁻⁶

The local velocity (interstitial) of fluid is estimated from the velocity at the entrance U_0 by

$$U_f = K \frac{U_0}{\varepsilon_i} \quad (10)$$

where K is a geometric factor that accounts for the tortuosity of the granular medium [9]. The value K is taken to 1.58. The particle porosity ε_i is estimated as follows

$$\varepsilon_i = 1 - 0.13N_b \text{ if } N_b \leq 4; \text{ otherwise } \varepsilon_i = 0.48 \quad (11)$$

where N_b is the number of contacts around the particle.

At the inlet, the air temperature is increased linearly from 200°C to 250°C in 200s then 250°C to 300°C in 1600s and is maintained at 300°C. The Nusselt number varies respectively with Reynolds number, Prandtl number and the porosity by an empirical correlation found in the literature as

$$Nu_i = \frac{h_f 2a_i}{\lambda_f} = (1 + 1.5(1 - \varepsilon_i)) \left(2 + 0.664 Re_i^{0.5} Pr^{1/3} \right) \quad (12)$$

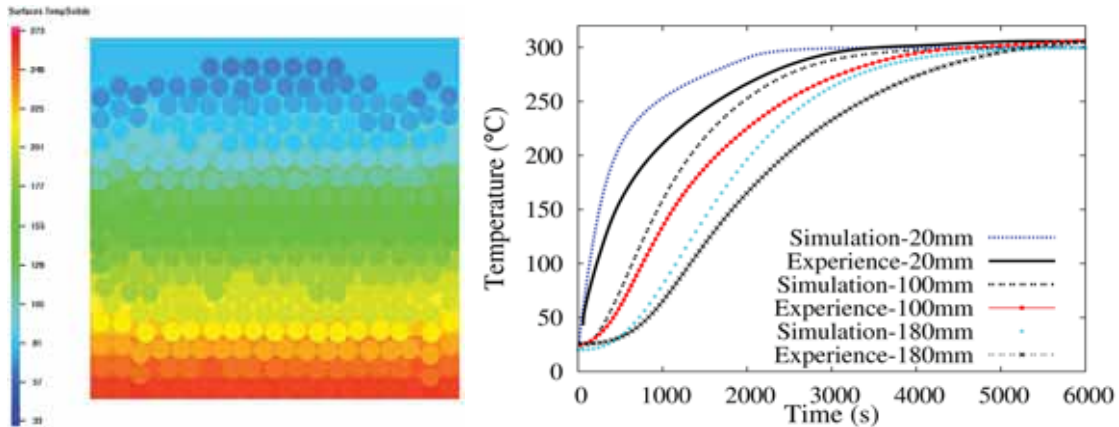


Fig 5. (a) Thermal map after 1000s (b) Heat evolutions

We show in Figure 5-a a thermal map thermal after 1000s. We observe a large temperature gradient between the inlet and the outlet box. The temperature field of the solid phase is not homogeneous. Figure 5-b shows the temperature evolutions at different heights in the granular bed. As expected by the experimental curves, the numerical results in Figure 5-b show almost identical curves for different positions of particles. A good experimental-numerical agreement is observed at the beginning and the end of these evolutions, a delay-time appears in transition phase.

In a second step, we study the cooling of a rectangular arrangement of granular hollow spheres ($5 \times 10 \times 5$ particles) whose experimental results are achieved by Laguerre *et al.* [10]. The granular bed has an initial temperature of 20°C. The cold air (0°C) is passing from left to the right of the system (Fig. 6). Note that in this simulation we have changed the modeled particle density to take into account the hollowness of experimental particles because the numerical particles are considered full.



Fig 6. Thermal map after 3600 s

The local Nusselt numbers is determined experimentally in function of particle rows (r_0) as

$$Nu = \frac{h_f 2a_i}{\lambda_f} = 1.56 \left(1 + 0.41 e^{-(r_0-1)/1.22} \right) Re_i^{0.42} Pr^{1/3} \quad (13)$$

The other parameters are detailed in the Table 4.

Table 4. Properties of the materials used in the simulation

Property	Value
Particle diameter [mm]	38.
Particle density [kg/m ³]	1000
Contact conductance [W/K]	0.0256
Particle heat capacity [J/(kg.K)]	4000
Air flow velocity [m/s]	0.11
Air temperature [°C]	20
Air heat conductivity [W/(m.K)]	0.0234
Air heat capacity [J/(kg.K)]	1055

Figure 7-a shows the temperature profile of our study and the profile of Laguerre *et al.* After an hour, a gap is observed near the inlet of cold air while the profiles converge at the outlet. In the Figure 7-b, we show the time variation of temperature of the middle particle of the first row (P1, from the left) and the last particle (P10). For the first, we see that the numerical evolution goes down asymptotically toward the steady-state (at 0.8 hour) faster than experimental curve. For the second (P10), a delay-time of predicted curve is observed. One supposes that this gap comes from the estimation of the coefficient of convective heat transfer.

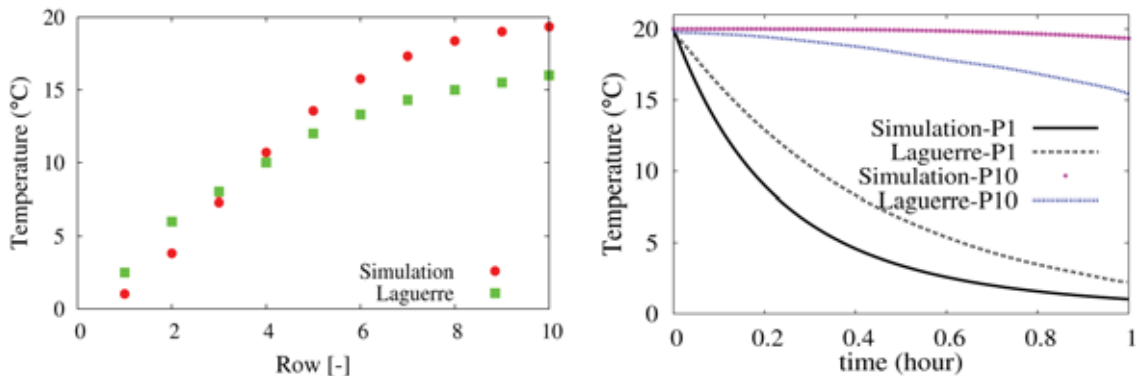


Fig 7. (a) Temperature in function of particle rows (b) Temperature variations over 1h cooling period

4. Conclusion

This paper examines the modeling of heat transfers in a granular system. Heat transfer by conductance in granular media has been fully validated. In this ideal case (conductance in vacuum), we have shown that the DEM is capable study the thermal exchange with maximum precision. For a biphasic medium, we showed various validations with experimental and numerical results reported in the literature. By using

experimental or empirical correlations of Nusselt numbers, we showed that our coupling can describe the thermal behaviour of interaction fluid/granular.

The next step will consist in the incorporation of the other heat phenomena like radiation. Moreover, further studies will focus on the three dimensional model. An experimental campaign is also planned to validate our thermal assumptions in dynamic behaviour.

References

- [1] Janas S, Malumba P, Deroanne C, Béra F. Comparaison d'un modèle empirique et d'un modèle physique de séchage de grains de maïs en lit fluidisé (in French). *Biotechnol Agron Soc Environ* 2010;**14**:389-398.
- [2] Tang Z, Cenkowski S, Muir WE. Modelling the superheated-steam drying of a fixed bed of brewers' spent grain. *Biosyst Eng* 2004;**87**:167–77.
- [3] Hager J, Wimmerstedt R, Whitaker S. Steam drying a bed of porous spheres: theory and experiment. *Chem Eng Sci* 2000;**55**:1675-1698.
- [4] Kato K, Ohmura S, Taneda D, Onozawa I, Shimura K, Iijima A. Drying characteristics in a packed fluidised bed dryer. *J Chem Eng Japan* 1981;**14**:365-371.
- [5] Vargas-Escobar WL. Discrete Modeling of Heat Conduction in Granular Media. Thesis. *University of Pittsburgh* 2002.
- [6] Simsek E, Brosch B, Wirtz S, Scherer V, Krüll F. Numerical simulation of grate firing systems using a coupled CFD/discrete element method (DEM). *Powder Technol* 2009;**193**:266–273.
- [7] Nguyen VD, Fortin J, Guessasma M, Bellenger E, Cogné C. Discrete modelling of granular flow with thermal transfer: application to the discharge of silos. *Appl Ther Eng* 2009;**29**:1846-1853.
- [8] Yun T, Santamarina J. Fundamental study of thermal conduction in dry soils. *Granular Matter* 2008;**10**:197–207.
- [9] Wen CY, Yu YH. Mechanics of fluidization. *Chem Eng Progr Symp* 1966;**62**:100-111.
- [10] Laguerre O, Ben Amara S, Flick D. Heat transfer between wall and packed bed crossed by low velocity airflow. *Appl Therm Eng* 2006;**26**:1951–1960.